Journal of Volcanology and Geothermal Research 217-218 (2012) 21–29

Contents lists available at SciVerse ScienceDirect

Journal of Volcanology and Geothermal Research

journal homepage: www.elsevier.com/locate/jvolgeores

Conductivity distribution beneath Lascar volcano (Northern Chile) and the Puna, inferred from magnetotelluric data

Daniel Díaz [a,c,*], Heinrich Brasse [a], Faustino Ticona [b]

[a] Freie Universität Berlin, Fachrichtung Geophysik, Malteserstr. 74-100, 12249 Berlin, Germany
[b] Universidad Mayor de San Andrés, La Paz, Bolivia
[c] Centro de Excelencia en Geotermia de Los Andes, Plaza Ercilla 803, Santiago, Chile

ARTICLE INFO

Article history:
Received 7 April 2011
Accepted 12 December 2011
Available online 29 December 2011

Keywords:
Magnetotellurics
Electrical conductivity
Volcanoes
Central Andes

ABSTRACT

During two field campaigns in 2007 and 2010, long-period and broadband magnetotelluric measurements were conducted in the Central Andes of northern Chile and northwestern Argentina at a latitude of 23.7°S. The study area spans from the Precordillera over the active volcanic arc of the Western Cordillera until the western part of the Puna. A special focus was on Lascar, a subduction related stratovolcano with an historical activity characterized by fumarolic emissions and occasional sub-plinian eruptions, like the one occurred on 1993. The broadband instruments, covering a period range between T = 0.005 s and 1000 s, were installed in the proximities of Lascar volcano, while the long-period devices (T = 10 s–10,000 s) were installed on a profile slightly south of Lascar, crossing the Salar de Atacama basin, the volcanic arc and reaching the western border of the Puna.

Remote reference and robust techniques were used for data processing. Induction vectors, phase tensor ellipses and strike direction of the conductivity distribution were calculated, showing some 3-D behavior for the Lascar sites at shallower depths, with induction vectors close to the edifice influenced partially by the topography. 3-D modeling and inversion revealed conductive anomalies beneath Lascar volcano, but also beneath the Puntas Negras volcanic chain. For the long-period transect, the behavior is closer to a 2-D case, with more stable strike direction coherent with induction vectors and phase tensor ellipses. The major result of 2-D inversion is a vast high-conductivity zone in the backarc crust, which seems to be the southern extension of a large highly conductive anomaly observed in prior studies beneath the Altiplano.

1. Introduction

The Central Andes have been formed in a long-lasting convergent system where, since Jurassic times, several oceanic plates were subducted under the South American plate. Subduction resulted in the formation of a magmatic arc that, due to tectonic erosion, has migrated about 200 km eastwards since 120 Ma, moving from the Coastal Cordillera to its present position in the Western Cordillera (Scheuber et al., 2006), comprising some of the highest peaks and the most active volcanoes of this mountain range. The volcanoes between 16° and 28° S are part of the Central Volcanic Zone (CVZ) of the Andes, characterized by steep subduction of the Nazca plate, with a subduction angle of nearly 30° at 100 km depth (Isacks, 1988), while north of 14° S and south of 28° S, the active volcanism vanishes, correlating with shallow subduction.

Volcanic-hydrothermal systems as well as magmatic sources are characterized by high electrical conductivity, and consequently form ideal targets for geophysical techniques sensitive to conductivity. Several magnetotelluric studies have been developed in different volcanic zones around the world during the last years, interpreting electrical conductors as hydrothermal fluids (e.g. Ingham et al., 2009), clays (e.g. Matsushima et al., 2001; Nurhasan et al., 2006) and also as magma conduits or chambers (e.g. Müller and Haak, 2004; Hill et al., 2009; Ingham et al., 2009).

In the Central Andes, Brasse et al. (2002) and Brasse and Eydam (2008) conducted long-period magnetotelluric investigations along two transects from the forearc to the Eastern Cordillera, crossing the volcanic arc of the Western Cordillera and the Altiplano high plateau (Fig. 1). One of the major findings was a large, highly-conductive anomaly in the mid-deep crust of the southern Altiplano at 21° S which was interpreted as a magmatic body with large amounts of partial melt. On the other hand, the deeper crust of the volcanic arc proper was not imaged as a good conductor. This is a rather surprising result considering a standard subduction scenario which predicts the rise of melts from the asthenospheric wedge. Note, however, that these previous studies were not focused on a specific arc volcano. This was the

* Corresponding author at: Universidad de Chile, Departamento de Geofísica, Blanco Encalada 2002, Santiago, Chile. Tel.: +56 2 9784295.
E-mail addresses: ddiaz@dgf.uchile.cl (D. Díaz), heinrich.brasse@fu-berlin.de (H. Brasse).

0377-0273/$ – see front matter © 2011 Elsevier B.V. All rights reserved.
doi:10.1016/j.jvolgeores.2011.12.007

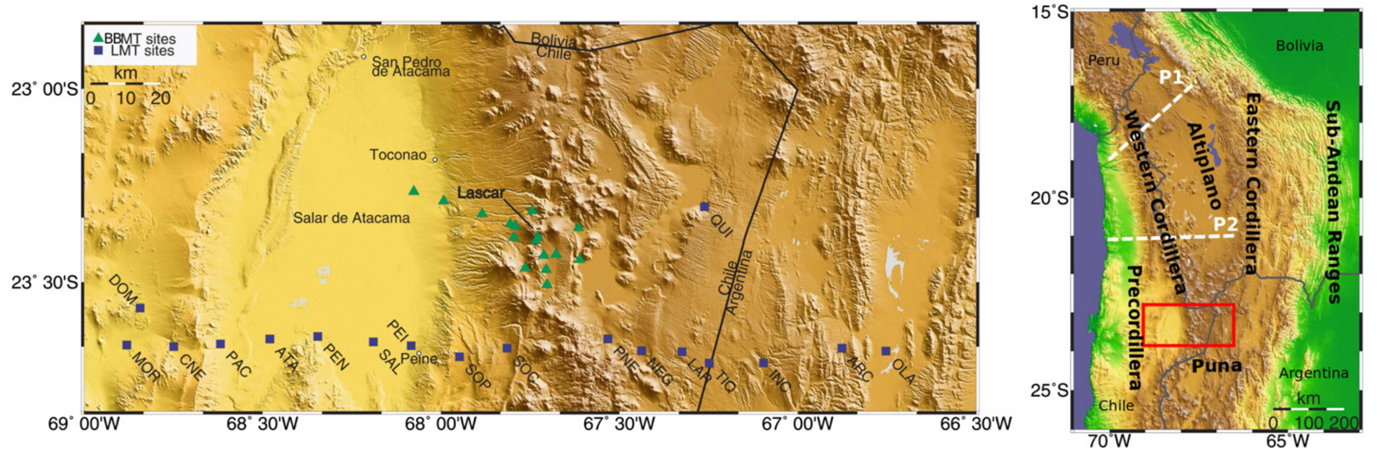

Fig. 1. Study zone and location of sites. Right: main geological features in the Central Andes. P1 and P2 represent two previous transects in this area by Brasse and Eydam (2008) and Brasse et al. (2002), respectively), and the red rectangle corresponds to the area shown in the figure to the left. Left: Detailed view around Lascar and the Salar de Atacama basin. LMT and BBMT locations are shown.

motivation for conducting a comparative transect further to the south and a more detailed study of a highly-active volcano of the Western Cordillera.

Magnetotelluric measurements, with broadband (BBMT) and long-period (LMT) equipment, were carried out between September and November 2007 and in a second field campaign during January–February 2010, setting stations in the vicinity of Lascar volcano (23°22′ S, 67°41′ W). This volcano, located on the western border of the Altiplano–Puna plateau, and sitting on a thickened crust with a Moho depth of nearly 70 km, is a typical example of a subduction-related volcano. Following the idea of an ascent of basaltic magmas produced in the upper mantle, due to the liberation of water from the subducted Nazca plate, and the subsequent emplacement of magmas of different compositions in the lower, middle and/or upper crust, the search for magma chambers, dyke-like structures or hydrothermal systems in the vicinity of this volcano constitutes the main aim of our investigation.

Due to the lack of roads and inaccessibility of remote eastern parts of the study area, the network around Lascar volcano couldn't be laid out in a regular, equidistant manner. With a summit height of 5592 m, Lascar is only one of the lower volcanoes in the vicinity, and the average altitude of site locations is well above 4000 m for the Western Cordillera and the Puna.

2. Regional geologic and tectonic setting

Between 18° and 23.5° S, the Central Andes are formed in a long-lasting convergent system where, since Jurassic times, the Farallon and later the Nazca plate, were subducted under the South American plate. Subduction resulted in the formation of a magmatic arc that, due to tectonic erosion, has migrated about 200 km eastwards since 120 Ma, moving from the Coastal Cordillera to its present position in the Western Cordillera (Scheuber et al., 2006).

In this zone, the Central Andes consist of major structural units which approximately parallel the trend of the mountain range. In the central part, where the Andes attain their maximum width, they comprise four regions, from west to east, (1) the offshore and onshore fore-arc region, (2) the Western Cordillera that marks the location of the presently active magmatic arc, (3) the Altiplano–Puna high plateau, and (4) an eastern belt of fold and thrust structures comprising the Eastern Cordillera and the Sub-Andean Ranges (Oncken et al., 2006).

Around 23°S, the Central Andean arc is retreated 60 km eastwards from its regional north-south trend, reaching a maximum distance from the Perú–Chile trench of about 400 km. To the west, the Central Andean arc is limited by the Salar de Atacama, a major topographic anomaly located at 2300 m above sea level, bordered to the west by the Cordillera de Domeyko as a subrange of the Precordillera. Crustal thickening that characterizes the backarc in this zone originated in Cenozoic times, particularly during the last 30 Ma (Allmendinger et al., 1997; Lamb, 2000). It coincides with an increase of relative convergence, which became almost orthogonal to the Chilean margin (Pardo-Casas and Molnar, 1987; Somoza, 1998), and with an eastward shift of magmatism (Coira et al., 1982). This was followed by the formation of Miocene–Pliocene stratovolcanoes, and led to the eruption of large-volume ignimbrites between 18° and 24°S. These ignimbrites constitute partly the basement over which several Pleistocene–Holocene volcanoes have been built. For an overview of the volcanic setting in this area see, e.g., de Silva (1989); de Silva and Francis (1991).

Lascar volcano, located on the eastern border of the Salar de Atacama basin (23.5° S), is active since less than 50 ka ago and has changed its activity center from time to time. The eastern edifice was created first with pyroxene-andesitic lavas, before the activity shifted to the west, where a rather large dome complex was produced, and which is now largely destroyed. The largest explosive episode (26.45 ka) produced 10–15 km^3 of mixed andesitic to dacitic pyroclastic flows and a large plinian fallout deposit (Soncor eruption), which was followed by another major explosive eruption (9.2 ka), and a new shift in the activity to the east, which is the currently active part of the volcano. New eruptions occurred around 7.1 ka ago, forming the Tumbres–Talabre lava (Matthews et al., 1997). Its historic activity has been recorded since 1848, and has been characterized by continuous fumarolic emissions and occasional sub-plinian eruptions, like the one in April 1993, which generated a column between 5 and 25 km high, collapse pyroclastic flows, and tephra falling over a large area of Paraguay, Uruguay, Brazil and Argentina.

3. LMT transect: two-dimensional model and interpretation

Long-period MT data at 18 locations were measured during field campaigns in September–October 2007 and January–February 2010 forming a profile, with a ~10 km separation between sites, which extends from the Cordillera de Domeyko, crossing the Salar de Atacama basin, the volcanic arc and reaching the Puna, following a W–E trend as can be seen in Fig. 1, which is approximately perpendicular to the main structural units. Due to the lack of roads the profile had to be shifted southward by ca. 30 km from the 3-D network around Lascar volcano, as described later.

Data have been analyzed to determine whether a consistent regional strike can be found for the whole profile using the algorithm of Smith (1995). Carrying out this analysis for the complete range of periods measured with the LMT stations, between 10 s and 10,000 s, the regional strike direction seems to be not unique. Developing the same analysis for the three decades of periods separately, it becomes clear that the data at short periods display a 3-D behavior, as the strike directions obtained for every station are very different from each other, especially in the forearc where the influence of the Salar de Atacama basin on nearby stations is very strong and where the Cordón de Lila range extends into the salar like a peninsula. However, a regional strike can be well determined for the period range between 100 s and 10,000 s with a value close to −10° from the north, i.e., N10°W.

These results are consistent with induction vectors, determined from the ratio of vertical to horizontal magnetic fields. They are plotted according to the convention of Wiese (1962), i.e. their real parts point away from conductors in a 2-D setting, and calculated for different periods of this profile (shown in Fig. 2). They indicate different directions for shorter periods and are particularly large at the borders of the Salar de Atacama basin. For longer periods, a common pattern is present in all the induction vectors, with a W–SW direction and similar lengths in the forearc, and decrease to almost zero on the Puna. This indicates already that a deep high conductivity anomaly is situated beneath the Puna, a result that is coincident with previous studies indicating the same kind of anomaly under the Bolivian Altiplano (Brasse et al., 2002; Brasse and Eydam, 2008).

The phase-sensitive skew of the impedance tensor, calculated according to the definition of Bahr (1988) is shown in Fig. 3. This parameter measures the phase difference between each pair of tensor elements and thus indicates a departure from the assumption of two-dimensionality. In the case of a perfect 2-D situation it will be zero, whereas values above ~0.3 can be considered as an indicator of true 3-D inductive regional structures. The same situation as for the induction vectors analysis is present, with a relatively high skewness for shorter periods at several stations. For periods around 100 s between stations PEI and SOP (the slope of the Western Cordillera), the rise of skewness until 0.3 could be related to the presence of intrusive rocks, a situation that will be discussed in the following sections. Apart from this feature, the values are mostly small and support the assumption of a 2-D Earth.

In order to overcome the effect of small-scale resistivity anomalies near the surface that distort the magnitude of the MT data, we also used the phase tensor (Caldwell et al., 2004) and its coordinate invariants to visualize the observed data. The phase tensor is defined by the relation

$$\Phi = Re(Z)^{-1} Im(Z), \quad (1)$$

where Φ is the phase tensor and Z the impedance tensor. According to Caldwell et al. (2004), the phase tensor, which is independent of galvanic distortions, can be represented graphically as an ellipse with the principal axes (Φ_{max} and Φ_{min}, respectively) showing the major and minor axes of the tensor. If the phase tensor is non-symmetric, a third coordinate invariant represented by the skew angle β is needed to characterize the tensor. Different cases can be represented by the phase tensor ellipses. For a uniform halfspace, a circle of unit radius represents the phase tensor at all periods. If the conductivity is both isotropic and 1-D, the radius of the circle will vary with period according to the variation of conductivity with depth. In a 2-D, or quasi 2-D, situation where β is zero or close to zero, respectively, the phase-tensor ellipse will have either its major or minor axes aligned with the geoelectric strike direction. Phase tensor ellipses for the LMT profile are shown in Fig. 4.

Following the previous arguments, a common electrical strike of N10°W was assumed, and all data were rotated by −10° into profile direction. Coastal effects are important only for very large periods, as the distance from the westernmost station to the coast is more than 150 km. We employed the non-linear conjugate gradient algorithm of Rodi and Mackie (2001) to carry out the 2-D inversion. Different starting models, including crude bathymetry (with ocean resistivity set to 0.3 Ωm) and a resistive subducted slab (ρ set to 1000 Ωm) were tested. Parameters controlling penalty on excessive horizontal or vertical structure were set to 1 (equal weight). As the LMT sites were sufficiently distant from topographic gradients (unlike the BBMT stations near Lascar volcano), topography was not included in the model. Variation of regularization parameters looking for a good

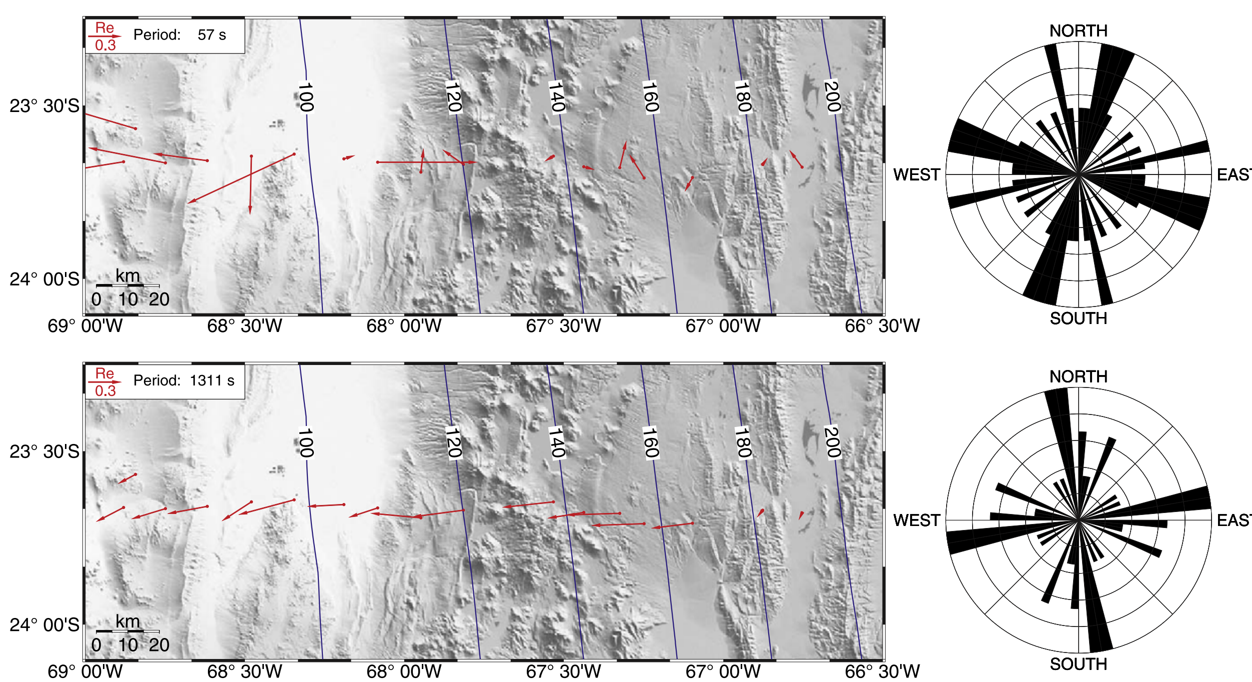

Fig. 2. Left side: Induction vectors for periods of 57 s (above) and 1311 s (below), the blue contour lines indicate depth in km of the Wadati–Benioff zone (Cahill and Isacks, 1992). Right side: strike directions for the period range 10 s–100 s (above), and 100 s–10,000 s (below).

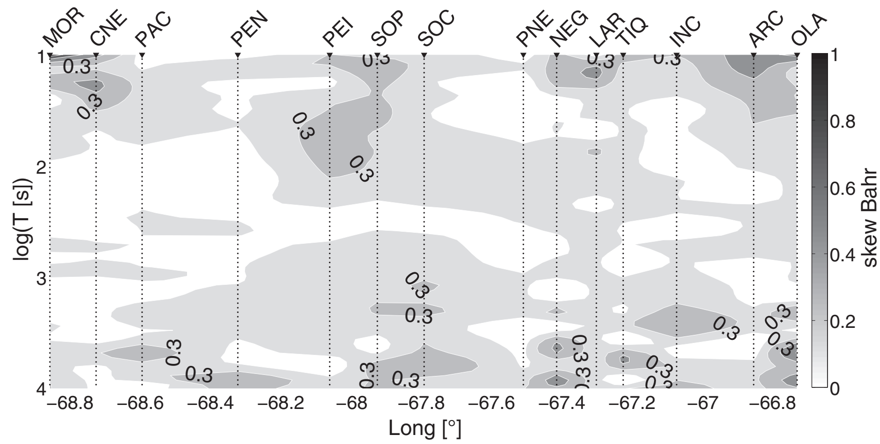

Fig. 3. LMT profile showing the phase sensitive skew in the definition of Bahr (1988). White and light tones indicate a skewness below 0.3, as a tentative measure for two-dimensionality.

trade-off between root mean square (RMS) fit and model roughness, and sensitivity tests of certain structures are some of the several experiments that were carried out in order to achieve a reliable model. For the resulting model (Fig. 5), obtained by jointly inverting tipper, TE and TM mode, we chose a regularization parameter of $\tau = 10$, because of the good trade-off between roughness and RMS fit. Error floors were set to 20% for apparent resistivities and 5° for phases, thus assigning a higher weight to phases in order to overcome the static shift problem.

Conductive and resistive features of the final model will be described now, starting with near-surface structures. The extremely high conductivity just below the surface of the Salar de Atacama (B in Fig. 5) is not surprising, since in-situ conductivity measurements in different water springs inside the salar showed values between 2.4 and 12.9 S/m at temperatures of ~25 °C (thus higher than the average of 3.3 S/m of sea water). The depth of this conductive zone varies through its extension. The eastern part extends from the surface until 1 or 2 km depth, while the western part reaches larger depths until ~5 km, as can be seen between stations PEN and PAC in Fig. 5. Studies including seismic lines across the Salar de Atacama indicate a considerable lateral variation in v_p depth distribution in the uppermost crust. A relatively high $v_p > 6.3$ km s^{-1} was found at shallower depths under the Cordón de Lila, surrounded to the east and west by a relatively low velocity zone (Reutter et al., 2006). This high velocity zone can be considered as the basement of the Salar

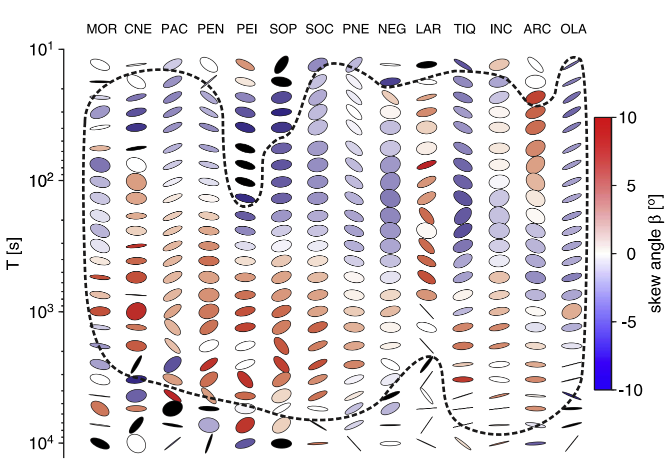

Fig. 4. Phase tensor ellipses for the LMT profile normalized by the maximum phase value, color scale represents β. The ellipses are plotted so that the horizontal axis corresponds to an east-west orientation. The segmented line encloses the ellipses with $|\beta| < 5°$.

de Atacama, constituted by Carboniferous and/or Permian to early Triassic volcanic and sedimentary successions partly penetrated by late Cretaceous plutons at the western, southern and southeastern borders of the Salar (Reutter et al., 2006). Between the Cordón de Lila and the El Bordo escarpment, several faults have been inferred based on geological data, gravity studies and seismic experiments. These structures, originally normal and then reversed as a result of the strong shortening experienced in this region during the Eocene and mid-Miocene, could be playing an important role for the infiltration of fluids into deeper levels in the southwestern zone of the Salar de Atacama. The importance of fluids in reversed fault systems has been analyzed in Ogawa et al. (2001). Another hypothesis for the deeper extension of the conductive zone to the west of the Cordón de Lila could be given by the origin of this tectonically depressed zone as a graben, supported by normal faults, which concentrated old lakes and evaporitic deposits which could explain a greater thickness of this kind of sediments, including perhaps horizons with fluids at depth (G. Chong, pers. comm.).

Another shallow structure, the resistive block marked as C in Fig. 5, can be related to the large skew values present between stations PEI and SOP, shown in Figs. 3 and 4. The 3-D effect suggested by the high skew values, together with the resistivities values obtained in the 2-D inversion could be related to the presence of crystalline intrusives in this part of the profile.

Considering the deeper structures, a large resistive block (C in Fig. 5) is observed below the westernmost stations. The large extension in depth of this unique block was tested comparing its model responses with the ones obtained with two highly resistive blocks separated by an average resistive layer, one extending above the Moho and the other one below it, obtaining slight differences between the two situations for stations MOR and CNE. The idea of two different highly resistive blocks comes from the two different sources for such an anomaly in this part of the profile at different depths: a crustal resistive block extending below the Cordillera de Domeyko, associated with plutons and crystalline intrusives observed at the surface, and a second one below the Moho, associated with the cold and strong subducted slab.

To the east, a large-scale conductive zone (structure D) located beneath the Puna and apparently extending to the upper mantle, presents resistivities as low as 1 Ωm. Several sensitivity tests were carried out in order to constrain the boundaries and extension of this conductive zone, setting its base at different depths by changing the low resistivities to values of 100 Ωm in the deeper part of the structure. As result, the RMS always increased, but as the deeper parts have only negligible influence on the model response, below 80 km we couldn't observe a clear increment in misfit. We thus consider

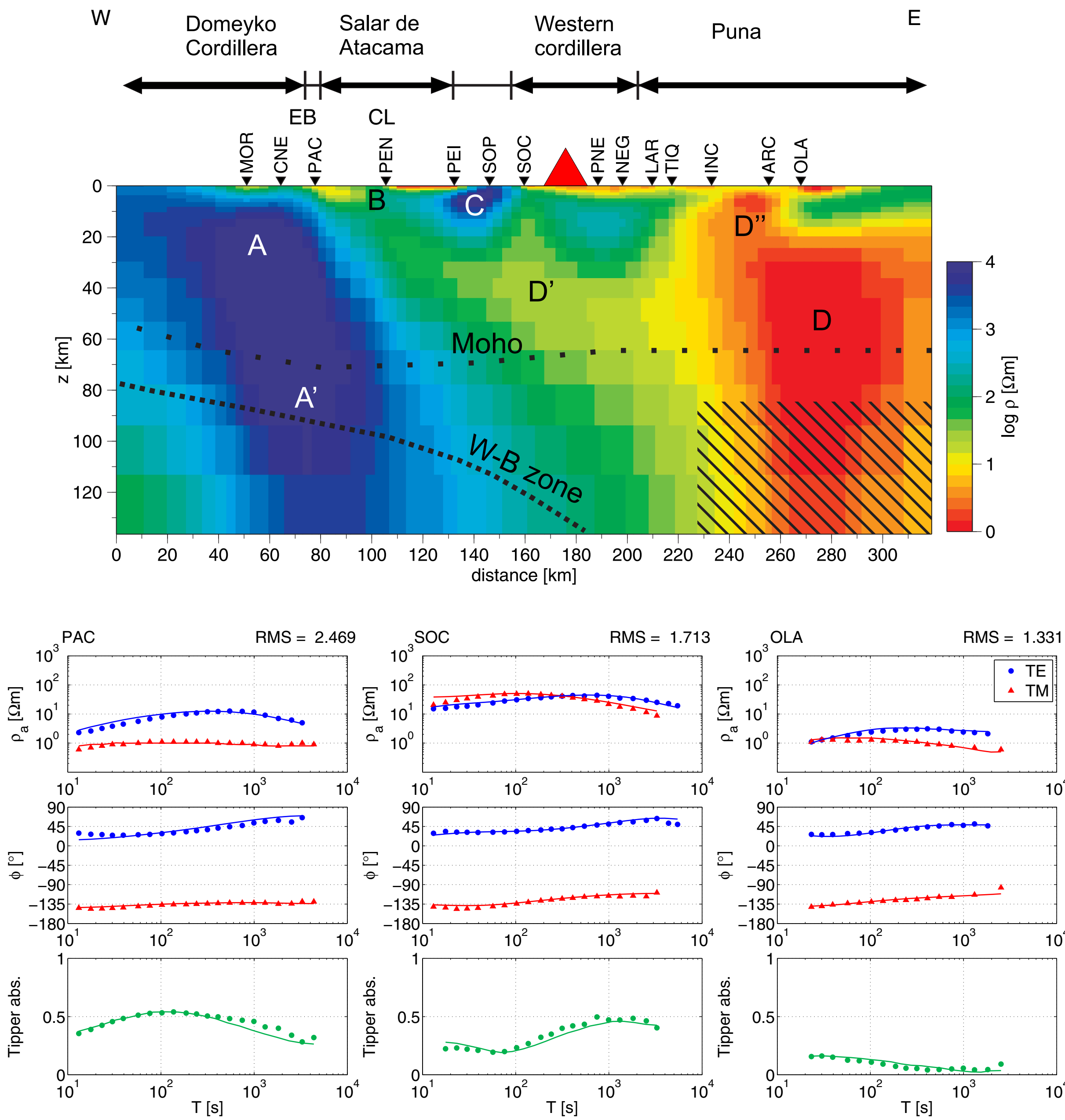

Fig. 5. 2-D inversion of the LMT profile using tipper, TE and TM modes; RMS: 1.957. The main geological features in the surface are indicated, together with the Moho which is roughly approximated from Yuan et al. (2000), and the Wadati–Benioff zone approximated from Cahill and Isacks (1992). EB marks the El Bordo escarpment, CL the Cordón de Lila range and the red triangle, the position of the volcanic arc. Below the 2-D inversion result, the comparison between measured (dotted lines) and modeled data (continuous lines) are shown for three stations representing the cases in the forearc (PAC), the volcanic arc (SOC) and the Puna (OLA). Error bars are smaller than symbol size.

the lower part of this conductive zone as unresolved (hatched area in Fig. 5). A less conductive structure which seems to escape from structure D (D′ in Fig. 5), enhances the conductivity just below the volcanic arc at depths of ~40 km. This relatively conductive zone was also subject to different experiments, testing its resolution and influence on the data. After replacing the low resistivities with normal values of 100 Ωm, the misfit was slightly increased at stations SOP, SOC and PNE. Running a new inversion with this setting, the structure D′ appears again after a few iterations. The lack of roads and adequate places for magnetotellurics where this profile crossed the Western Cordillera plays against a better resolution of the conductive structures beneath this part of the volcanic arc. However the BBMT data measured 30 km north of this profile, around one particular volcano of the Western Cordillera, could give some hints about the conductive structure beneath the volcanic arc of this part of the Andes. These results are shown in the next section.

The highly conductive zone below the Puna, extending from the mid-lower crust to the upper mantle, is in good agreement with the idea of melts produced in the asthenospheric wedge above the subducted plate, even when this conductive anomaly is located not beneath the volcanic front but shifted ~100 km to the east. The presence of this conductive anomaly starting at mid-crustal levels is interesting considering the suggestion of a shallow brittle–ductile transition beneath the Puna, due to a crustal seismicity which is restricted to small depths (<10 km) (Asch et al., 2006). Laterally, the conductive anomaly beneath the Puna matches with the southern extension of the Altiplano–Puna magma body (APMB), as inferred from a seismic very low velocity zone (v_s) by Chmielowski et al. (1999).

According to receiver function analysis by Zandt et al. (2003), this anomaly extends from 17 to 19 km depth with a thickness of only 1–2 km. In contrast, the high conductivity zone (HCZ) must extend much deeper in order to fit the measured data, as can be seen in the sensitivity test included in the supporting material. Petrological and geochemical data suggest that magmas related to ignimbrites in the Altiplano–Puna volcanic complex were formed from a mixture of mantle and crustal melts at depths between 30 and 15 km (de Silva et al., 2006). The deeper extension of the highly conductive anomaly beneath the Puna could be related to the ascent of the mantle melts from the upper mantle through the lower crust, until depths of ~20 km, where they accumulate forming low velocity and highly conductive zones.

The hypothesis of large volumes of partial melt in the mid-lower crust to upper mantle is supported by the low seismic velocities and Q_p values observed in the same area by Schurr et al. (2006). Furthermore, the Puna conductor resembles the high conductivity zone beneath the southern Altiplano at 21°S (Brasse et al., 2002; Schilling et al., 2006) with respect to its depth and location in the backarc. Encompassing almost the entire mid-lower crust, this Altiplano HCZ correlates very well with the low velocity zone described by Heit et al. (2008) beneath the same profile. The crustal conductor is missing further to the north at 17.5°S beneath the central Altiplano, which enabled Brasse and Eydam (2008) to resolve the source region in the asthenospheric wedge. Summarizing, all these observations are also consistent with dehydration-related earthquakes located deeper than usual, i.e., at up to 200 km depth.

4. Three-dimensional modeling of Lascar data

A dimensionality analysis was also performed with the data from the broadband stations, considering a much wider period range (0.004 s–1000 s) than in the LMT case. At first sight, no large conductive anomaly under Lascar volcano could be inferred from the analysis of the induction vectors of the surrounding stations. Induction vectors and phase tensor ellipses for the BBMT data are shown in Fig. 6. For the shortest periods, the topography plays an important role: at stations close to the volcanic edifice, induction vectors point away from it. However, for the period range between 1 s and 30 s, the BBMT stations show a behavior which indicates a conductive anomaly in the S–SE of Lascar volcano, where small induction vectors are surrounded by larger ones pointing away from this zone, as can be seen in Fig. 6. This corresponds to Φ_{min} values above 45° in this area S–SE of the volcano. At periods between 0.1 s and 1 s this behavior is also present at stations directly at the southern slope of the volcanic edifice, and to the stations southwards. Beyond 1 s, until almost 10 s, Φ_{min} becomes slowly smaller for the stations closer to the volcano (L07 and L08), but the stations to the south are still showing higher values. This is again indicating the presence of a highly conductive zone to the south of the volcano, and probably reaching larger depths at its southern margins.

For the BBMT data it was not possible to define a common strike for periods shorter than 100 s. Only for the largest period range, between 100 s and 1000 s a strike direction similar to the one obtained for the LMT data is clearly defined. As has been pointed out by the dimensionality indicators analyzed here, the largest part of this data set cannot be interpreted as two-dimensional, and therefore a three-dimensional interpretation for the BBMT data measured around Lascar volcano is needed.

3-D forward modeling was performed with the program developed by Mackie et al. (1994) for the closest sites around Lascar volcano, trying to find the synthetic model which fits the measured data best. E.g., models including a highly conductive zone (1 Ωm, simulating a magma deposit) placed at 5, 10 and 15 km depth under the volcanic edifice, with different shapes and sizes were tested, obtaining poor fit for the off-diagonal elements of the impedance tensor and tipper. The presence of conductors directly beneath the volcano seems to be limited to 2 or 3 km under the surface, which accounts more likely for a hydrothermal system rather than a magma chamber, coinciding with tremor observations related to steam or gases in the direct

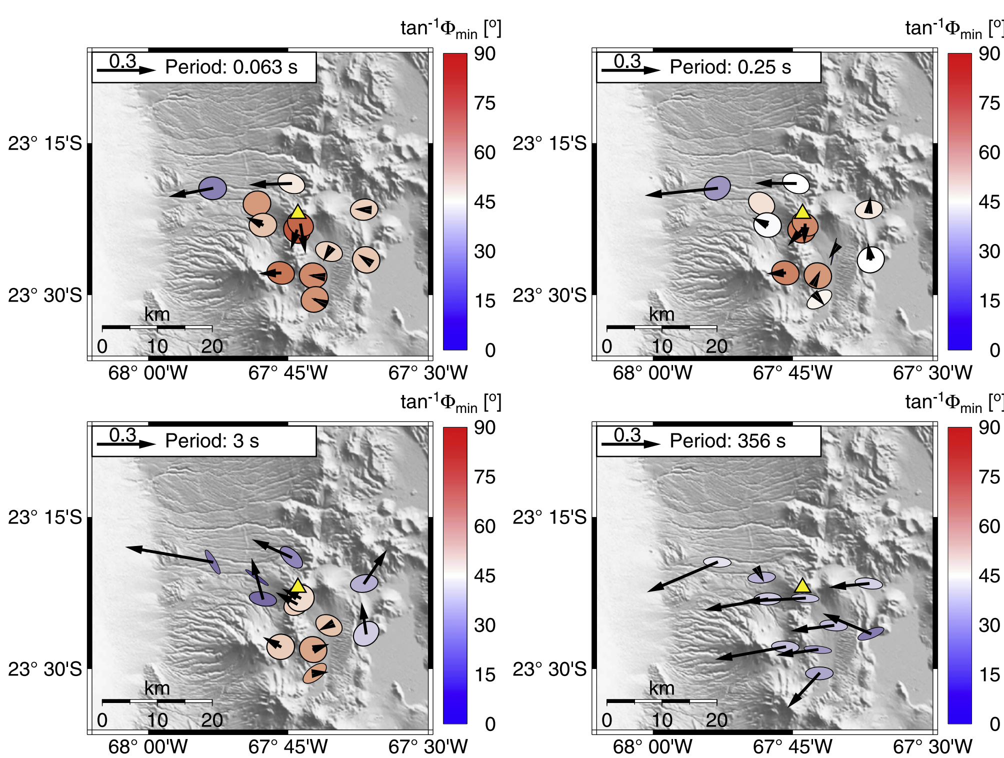

Fig. 6. Real part of the induction vectors and phase tensor ellipses for the BBMT stations around Lascar volcano, marked as a yellow triangle. The color scale is indicating the value of Φ_{min}.

vicinity of the volcano (Hellweg, 1999, 2000). Instead, a conductive zone has to be included south to the edifice of Lascar, in direction toward Chiliques volcano – such a conductor enhances the data fit substantially, in particular for the tipper. The best-fitting model which has been found by forward modeling, and which includes several other conductive features, is shown in the electronic supplement.

Other features needed by the magnetotelluric data are a resistive and relatively shallow block at the eastern border of the Salar de Atacama, associated with intrusives present in the Cuyuguas and Allana hills, and some other shallow conductors, associated with the Aguas Calientes Salar, to the east of Lascar volcano.

As 3-D modeling is a tedious affair, particularly if several anomalies are present, we additionally applied the 3-D inversion code of Siripunvaraporn et al. (2005). This program was extended and implemented from the 2-D data space Occam's inversion (Siripunvaraporn and Egbert, 2000), seeking the minimum structure model subject to an appropriate fit to the data. The difficulties associated with the use of Occam's approach to 3-D MT inversion, due to the size of the model parameter M, can be overcome with a data space approach, where matrix dimensions depend on the size of the data set N, rather than M. As in general $N \ll M$ for MT data, as discussed in Siripunvaraporn et al. (2005), the transformation of the inverse problem to data space can significantly improve the computational efficiency, making the 3-D inversion practical for normal PCs.

Note that this code does not invert for tipper transfer function and does not support topography. In mountainous terrain this limits the applicability to periods $T>1$ s, since severe topography effects dominate at shorter periods, which may result in a false conductor beneath the volcano edifice.

In order to efficiently use the 3-D inversion program, a subset of the data was chosen, excluding sites with poor data quality and selecting only 3 periods per decade, thus reducing the size of the data (N) and therefore memory size and CPU time. The size of the model (M) was given by the discretization of the area of interest around Lascar volcano, with a cell size in the central part of the grid of $1000 \times 1000 \times 500$ m in x, y and z directions, respectively. This grid is coarser as the one used for the 3-D forward modeling, but with finer grids the program did not run on a 4 GB RAM computer. The inversion result shown in Figs. 7 and 8 was obtained inverting the full impedance tensor for 12 BBMT stations, setting an error floor of 10% to the data, and starting from an homogeneous half space of 100 Ωm. The data fit for 4 stations is shown in Fig. 7, while for the whole data set an RMS = 2.057 was obtained.

Similar results as in the forward modeling study were obtained, particularly the conductive structure extending to the south of the volcanic edifice, and reaching larger depths (6 km) at its southern margin, ~15 km south of Lascar. This conductive zone is located in the middle of several volcanic centers, limited to the north by Lascar and Aguas Calientes volcanoes, and to the south by the Puntas Negras volcanic chain and Chiliques volcano. Note, that the latter has displayed thermal activity in recent years (http://earthobservatory.nasa.gov/NaturalHazards/view.php?id=9419, retrieved 02 December 2011).

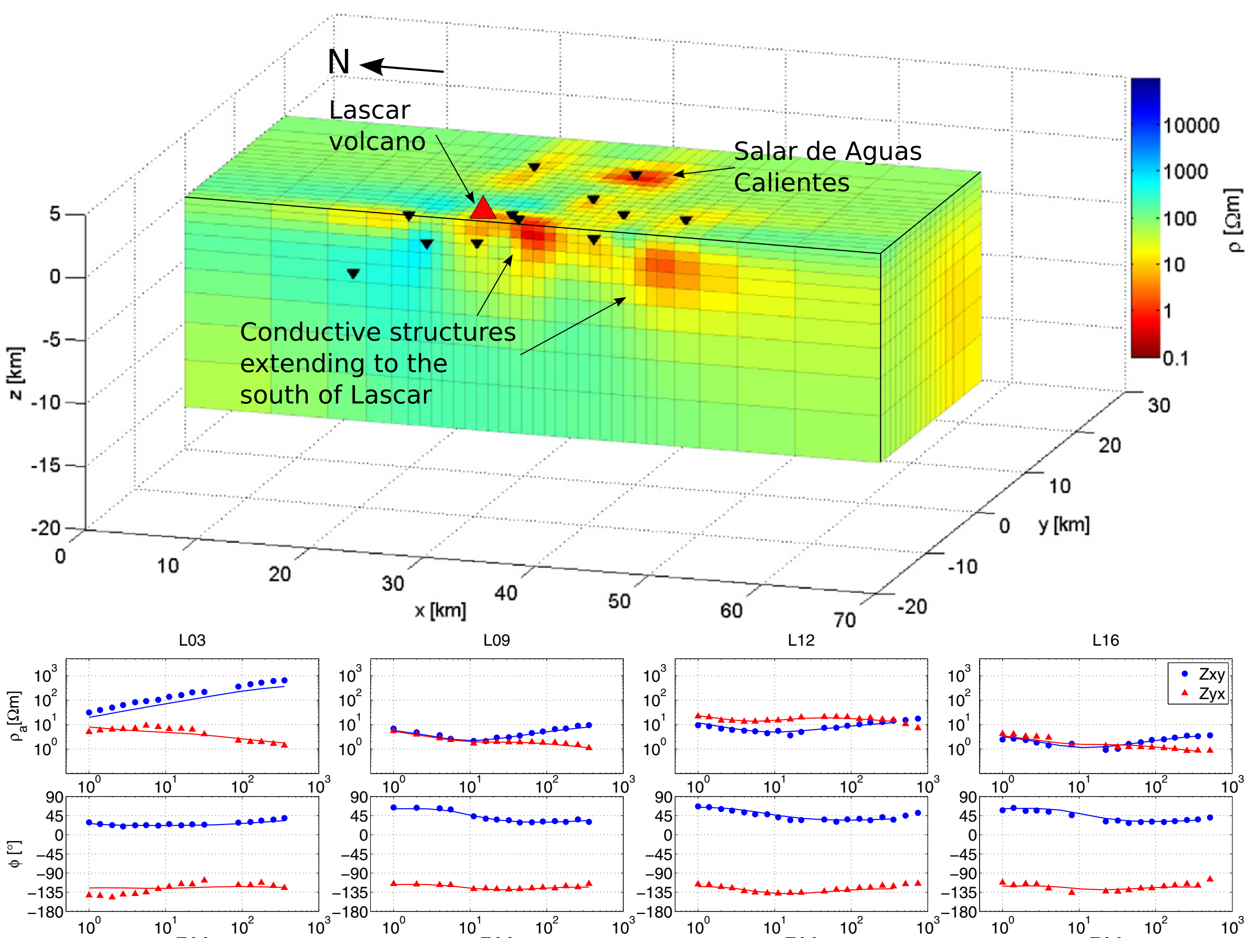

Fig. 7. Top: result of a 3-D inversion for the Lascar volcano area, view from the W–SW. RMS = 2.057 considering data from the full impedance tensor for 12 stations around Lascar volcano (black triangles). Bottom: comparison between measured (dotted lines for app. resistivity and phase, for both the off-diagonal elements of the impedance tensor) and modeled data (continuous lines for app. resistivity and phase) for four stations around Lascar volcano. Error bars are smaller than symbol size.

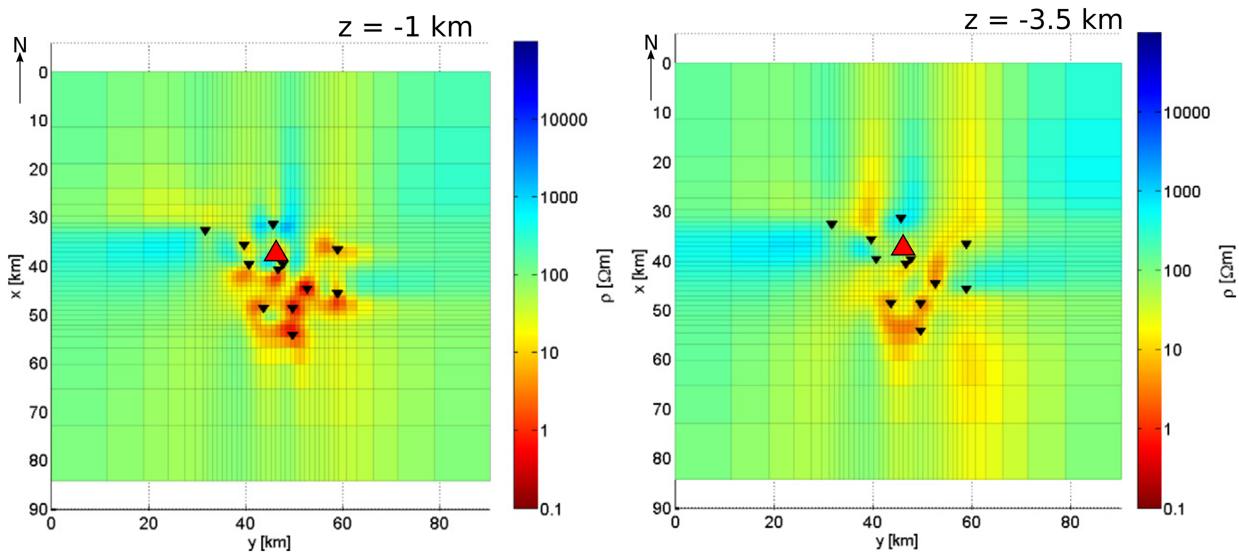

Fig. 8. Two slices at a fixed depth of the same 3-D inversion shown in Fig. 7. Left: Slice at 1 km depth. Right: Slice at 3.5 km depth. Lascar volcano is shown as a red triangle and BBMT stations as black triangles for reference.

5. Conclusions

2-D inversion of the long-period transect yields a model, which largely agrees with the main tectonic features in this area. The subducting slab together with a crustal block coinciding with the Cordillera de Domeyko were modeled as highly resistive zones, while the Salar de Atacama, extending a few kilometers in depth, was resolved as a very conductive area, which agrees with in-situ conductivity measurements. A large highly conductive anomaly (~1 Ωm) was obtained beneath the Puna, starting at 10–20 km depth, and probably extending through the Moho. The presence of such an anomaly fits well with previous conductivity models obtained beneath the Altiplano to the north (Brasse et al., 2002; Brasse and Eydam, 2008). A relatively conductive anomaly (20–30 Ωm) was also obtained below the active volcanic arc at depths between 10 and 30 km. These conductive anomalies, both associated with seismicity clustered beneath at the plate interface, are possibly related to dehydration processes of the subducting slab. The ascending fluids lead to melting of the mantle wedge and further rise into the crust.

These anomalies beneath the arc and the backarc agree also with seismic tomography results in this area (Schurr et al., 2006). The larger and more conductive anomaly located beneath the plateau is possibly related to the processes originating the young monogenetic volcanic centers associated with mafic lavas in the Puna, such as Tuzgle volcano and shoshonitic lavas. They are derived from the ascent of mantle material, contaminated by mixing with crustal melts in the lower crust, according to Coira and Kay (1993), and coinciding with the depth extent and location of the larger anomaly. The mantle at the base of the crust, probably causing partial melt in the lower crust, may be the cause of a conductive anomaly at crustal–mantle depths, enhancing the ascent of magma through the crust, that may accumulate at crustal depths in the backarc as in the APMB (Zandt et al., 2003) or the ALVZ (Heit et al., 2008) and be the source for large ignimbrite deposits observed in this zone, or ascend through a more direct-path, such in the case of Tuzgle volcano. A direct, conductive link of Tuzgle volcano to the mantle was already proposed by Lezaeta and Brasse (2001), even though the present study with LMT stations cannot resolve such small features.

Speculatively, the observation of a larger and more conductive anomaly located beneath the backarc instead of beneath the main volcanic arc in the Western Cordillera, could be a snapshot of the eastward migration of the arc, as it has occurred already several times since the Jurassic.

The presence of a highly conductive zone beneath the Puna, as well as in the northern part of the plateau, beneath the Altiplano, suggest that this feature is common to almost the entire plateau, but showing some remarkable differences beneath the Altiplano and the Puna. Beneath the Altiplano, this highly conductive zone starts at larger depths and is also extending until ~120 km, while beneath the Puna this feature is starting and probably finishing at shallower depths.

The high conductivity zone beneath the Puna fits with previous studies showing similar results in other parts of the plateau. The different depth extensions of the highly conductive zones beneath the two segments of the plateau can be associated with a thinner lithosphere beneath the Puna, which is approximately 50 km thicker beneath the Altiplano (Whitman et al., 1992), and therefore with the morphological differences observed between the higher and narrower Puna and the lower, wider and thick-crusted Altiplano.

A magma chamber was not resolved by 3-D modeling and inversion beneath Lascar volcano. A conductive layer beneath the summit rather hints at fluids of hydrothermal system. A similar conductive layer is observed in the Salar de Aguas Calientes, probably due to the saline fluids and thermal springs present in this Salar. Both conductive layers are of shallow extension (no more than 1 km depth according to Fig. 8). Instead, a conductive zone extending to the south of Lascar, reaching depths of 6 km beneath the surface at its southern margin was modeled. This conductive zone could be related to the presence of fluids and/or magma, forming a feeding zone for other volcanic centers in this area. Note, that the foregoing results do not exclude a magma chamber and/or conduit of minor dimensions directly beneath the Lascar edifice, which would be difficult to resolve, however.

Acknowledgments

Thanks to the German and Chilean students who helped us during the field campaigns in 2007 and 2010. We thank G. Chong and H. Wilke (Universidad Católica del Norte, Antofagasta), C. Pomposiello and A. Favetto (Universidad de Buenos Aires) for help in logistical issues, and the German Embassy Buenos Aires for customs clearance in Argentina. We are grateful to E. Medina (Antofagasta), to the working groups of F. Holtz (Leibniz Universität Hannover) and of G. Wörner (Universität Göttingen) for discussions and information regarding the petrological and geochemical results of their measurements in the Lascar volcano area. V. Siripunvaraporn provided the 3-D inversion code. Most plots were prepared with the GMT package of Wessel and

Smith (1998). This work was funded by German Research Foundation (DFG).

Appendix A. Supplementary data

Supplementary data to this article can be found online at doi:10.1016/j.jvolgeores.2011.12.007.

References

Allmendinger, R.W., Jordan, T.E., Kay, S.M., Isacks, B.L., 1997. The evolution of the Altiplano–Puna plateau of the Central Andes. Annual Review of Earth and Planetary Sciences 25, 139–174.

Asch, G., Schurr, B., Bohm, M., Yuan, X., Haberland, C., Heit, B., Kind, R., Woelbern, I., Bataille, K., Comte, D., Pardo, M., Viramonte, J., Rietbrock, A., Giese, P., 2006. Seismological studies of the Central and Southern Andes. In: Oncken, O., et al. (Ed.), The Andes: Active Subduction Orogeny, Frontiers in Earth Sciences. Springer, Berlin, pp. 443–457.

Bahr, K., 1988. Interpretation of the magnetotelluric impedance tensor: regional induction and local telluric distortion. Journal of Geophysics 62, 119–127.

Brasse, H., Eydam, D., 2008. Electrical conductivity beneath the Bolivian Orocline and its relation to subduction processes at the South American continental margin. Journal of Geophysical Research 113, B07109. doi:10.1029/2007JB005142.

Brasse, H., Lezaeta, P., Rath, V., Schwalenberg, K., Soyer, W., Haak, V., 2002. The Bolivian Altiplano conductivity anomaly. Journal of Geophysical Research 107, B5. doi:10.1029/2001JB000391.

Cahill, T., Isacks, B., 1992. Seismicity and Shape of the Subducted Nazca Plate. Journal of Geophysical Research 97 (B12), 17503–17529. doi:10.1029/92JB00493.

Caldwell, T.G., Bibby, H.M., Brown, C., 2004. The magnetotelluric phase tensor. Geophysical Journal International 158, 457–469.

Chmielowski, J., Zandt, G., Haberland, C., 1999. The Central Andean Altiplano–Puna Magma body. Geophysical Research Letters 26, 783–786.

Coira, B., Kay, S., 1993. Implications of Quaternary volcanism at Cerro Tuzgle for crustal and mantle evolution of the Puna Plateau, Central Andes, Argentina. Contributions to Mineralogy and Petrology 113, 40–58.

Coira, B., Davidson, J., Mpodozis, C., Ramos, V., 1982. Tectonic and magmatic evolution of the Andes of northern Argentina and Chile. Earth-Science Reviews 18, 303–332.

de Silva, S.L., 1989. Altiplano–Puna volcanic complex of the Central Andes. Geology 17, 1102–1106.

de Silva, S.L., Francis, P.W., 1991. Volcanoes of the Central Andes. Springer-Verlag, New York.

de Silva, S.L., Zandt, G., Trumbull, R., Viramonte, J.G., Salas, G., Jimenez, N., 2006. In: Troise, C., De Natale, G., Kilburn, C.R.J. (Eds.), Mechanisms of Activity and Unrest at Large Calderas: Geological Society, London, Special Publications, 269, pp. 47–63.

Heit, B., Koulakov, I., Asch, G., Yuan, X., Kind, R., Alcocer-Rodriguez, I., Tawackoli, S., Wilke, H., 2008. More constraints to determine the seismic structure beneath the Central Andes at 21°S using teleseismic tomography analysis. Journal of South American Earth Sciences 25. doi:10.1016/j.jsames.2007.08.009.

Hellweg, M., 1999. Seismic signals from Lascar Volcano. Journal of South American Earth Sciences 12, 123–133.

Hellweg, M., 2000. Physical models for the source of Lascar's harmonic tremor. Journal of Volcanology and Geothermal Research 101, 183–198.

Hill, G., Caldwell, T.G., Heise, W., Chertkoff, D.G., Bibby, H.M., Burgess, M.K., Cull, J.P., Cas, R.A.F., 2009. Distribution of melt beneath Mount St Helens and Mount Adams inferred from magnetotelluric data. Nature Geoscience 2 (11), 785–789.

Ingham, M.R., Bibby, H.M., Heise, W., Jones, K.A., Cairns, P., Dravitzki, S., Bennie, S.L., Caldwell, T.G., Ogawa, Y., 2009. A Magnetotelluric study of Mount Ruapehu volcano, New Zealand. Geophysical Journal International 179, 887–904.

Isacks, B.L., 1988. Uplift of the central Andean plateau and bending of the Bolivian Orocline. Journal of Geophysical Research 93, 3211–3231.

Lamb, S., 2000. Active deformation in the Bolivian Andes, South America. Journal of Geophysical Research 105, 627–653.

Lezaeta, P., Brasse, H., 2001. Electrical conductivity beneath the volcanoes of the NW Argentinian Puna. Geophysical Research Letters 28, 4651–4654.

Mackie, R.L., Smith, J.T., Madden, T.R., 1994. Three-dimensional electromagnetic modeling using unite difference equations: the magnetotelluric example. Radio Science 29, 923–935.

Matsushima, N., Oshima, O., Ogawa, Y., Takakura, S., Satoh, H., Utsugi, M., Nishida, Y., 2001. Magma prospecting in Usu volcano, Hokkaido, Japan, using magnetotelluric soundings. Journal of Volcanology and Geothermal Research 109, 263–277.

Matthews, S.J., Gardeweg, M.C., Sparks, R.S.J., 1997. The 1984 to 1996 cyclic activity of Lascar Volcano, northern Chile: cycles of dome growth, dome subsidence, degassing and explosive eruptions. Bulletin of Volcanology 59, 72–82. doi:10.1007/s004450050176.

Müller, A., Haak, V., 2004. 3-D modelling of the deep electrical conductivity of Merapi volcano (Central Java): integrating magnetotellurics, induction vectors and the effects of steep topography. Journal of Volcanology and Geothermal Research 138, 205–222.

Nurhasan, Ogawa, Y., Ujihara, N., Tank, S.B., Honkura, Y., Onizawa, S., Mori, T., Makino, M., 2006. Two electrical conductors beneath Kusatsu-Shirane volcano, Japan, imaged by audiomagnetotellurics, and their implications for the hydrothermal system. Earth Planets Space 58, 1055–1059.

Ogawa, Y., Mishina, M., Goto, T., Satoh, H., Oshiman, N., Kasaya, T., Takahashi, Y., Nishitani, T., Sakanaka, S., Uyeshima, M., Takahashi, Y., Honkura, Y., Matsushima, M., 2001. Magnetotelluric imaging of fluids in intraplate earthquake zones, NE Japan back arc. Geophysical Research Letters 28, 3741–3744.

Oncken, O., Hindle, D., Kley, J., Elger, K., Victor, P., Schemmann, K., 2006. Deformation of the Central Andean upper plate system–facts, fiction, and constraints for plateau models. In: Oncken, O., et al. (Ed.), The Andes: Active Subduction Orogeny, Frontiers in Earth Sciences. Springer, Berlin, pp. 3–27.

Pardo-Casas, F., Molnar, P., 1987. Relative motion of the Nazca (Farallon) and South American plates since Late Cretaceous time. Tectonics 6, 233–248.

Reutter, K.J., Charrier, R., Götze, H.J., Schurr, B., Wigger, P., Scheuber, E., Giese, P., Reuther, C.D., Schmidt, S., Rietbrock, A., Chong, G., Belmonte-Pool, A., 2006. The Salar de Atacama Basin: a Subsiding Block within the Western Edge of the Altiplano–Puna Plateau. In: Oncken, O., et al. (Ed.), The Andes: Active Subduction Orogeny, Frontiers in Earth Sciences. Springer, Berlin, pp. 303–325.

Rodi, W., Mackie, R.L., 2001. Nonlinear conjugate gradients algorithm for 2-D magnetotelluric inversions. Geophysics 66, 174–187.

Scheuber, E., Mertmann, D., Harald, E., Silva-Gonzalez, P., Heubeck, C., Reutter, K.J., Jacobshagen, V., 2006. Exhumation and basin development related to formation of the central Andean plateau, 21°S. In: Oncken, O., et al. (Ed.), The Andes: Active Subduction Orogeny, Frontiers in Earth Sciences. Springer, Berlin, pp. 285–301.

Schilling, F.R., Trumbull, R.B., Brasse, H., Haberland, C., Asch, G., Bruhn, D., Mai, K., Haak, V., Giese, P., Muñoz, M., Ramelow, J., Rietbrock, A., Ricaldi, E., Vietor, T., 2006. Partial melting in the Central Andean crust: a review of geophysical, petrophysical, and petrologic evidence. In: Oncken, O., et al. (Ed.), The Andes: Active Subduction Orogeny, Frontiers in Earth Sciences. Springer, Berlin, pp. 459–474.

Schurr, B., Rietbrock, A., Asch, G., Kind, R., Oncken, O., 2006. Evidence for lithospheric detachment in the central Andes from local earthquake tomography. Tectonophysics 415, 203–223.

Siripunvaraporn, W., Egbert, G., 2000. An efficient data-subspace inversion method for 2-D magnetotelluric data. Geophysics 65, 791–803.

Siripunvaraporn, W., Egbert, G., Lenbury, Y., Uyeshima, M., 2005. Three-dimensional magnetotelluric inversion: data-space method. Physics of the Earth and Planetary Interiors 150, 3–14.

Smith, J.T., 1995. Understanding telluric distortion matrices. Geophysical Journal International 122, 219–226.

Somoza, R., 1998. Updated Nazca (Farallon)-South America relative motions during the last 40 My: implications for mountain building in the central Andean region. Journal of South American Earth Sciences 11, 211–215.

Wessel, P., Smith, W.H.F., 1998. New, improved version of the generic mapping tools released. EOS. Transactions of the American Geophysical Union 79, 579.

Whitman, D., Isacks, B.L., Chatelain, J.L., Chiu, J.M., Perez, A., 1992. Attenuation of high-frequency seismic waves beneath the central Andean plateau. Journal of Geophysical Research 97, 19929–19947.

Wiese, H., 1962. Geomagnetische Tiefentellurik Teil II: die Streichrichtung der Untergrundstrukturen des elektrischen Widerstandes, erschlossen aus geomagnetischen Variationen. Pure and Applied Geophysics 52, 83–103.

Yuan, X., Sobolev, S.V., Kind, R., Oncken, O., Bock, G., A., G., Schurr, B., Graeber, F., Rudloff, A., Hanka, W., Wylegalla, K., Tibi, R., Haberland, C., Rietbrock, A., Giese, P., Wigger, P., Röwer, P., Zandt, G., Beck, S., Wallace, T., Pardo, M., Comte, D., 2000. Subduction and collision processes in the Central Andes constrained by converted seismic phases. Nature 408, 958–961.

Zandt, G., Leidig, M., Chmielowski, J., Baumnot, D., Yuan, X., 2003. Seismic detection and characterization of the Altiplano–Puna magma body, Central Andes. Pure and Applied Geophysics 160, 789–807.